Original Research Article

WELL BASED ELASTIC ATTRIBUTE ANALYSIS FOR RESERVOIR CHARACTERIZATION IN EK-FIELD NIGER DELTA

ABSTRACT

Derived elastic attributes study has been used to discriminate rock and fluid properties in EK Field using well logs data.These derived rock attributes were analysedin cross-plot space for target reservoirs.The log analysis for delineated reservoir B20 shows an average volume of shale (7.5%), total porosity (33.9%) and water saturation (29.3%). Cross-plots ofelastic rock attributes (Vp/Vs, Lambda-Rho (λρ), Mu-Rho (μρ), Poisson ratio and acoustic impedance) were used as fluid and lithology indicators and in reservoir characterization.Thecrossplots results shows distinct separation of hydrocarbon sand, brine sand and shale. Low Poisson's ratio (0.2-0.26), Lambda-Rho (7 GPa*g/cc -10 GPa*g/cc), Vp/Vs (1.6-1.8), low acoustic impedance and high Mu-Rho values indicate hydrocarbon sands. The intermediate values of Poisson's ratio (0.2-0.26), Lambda-Rho(17 GPa*g/cc - 21GPa*g/cc) , Vp/Vs ratio (2.05-2.3), relatively high acoustic impedance and Mu-rho indicated brine sand while high Poisson's ratio (0.35-0.41), Lambda-rho (24 GPa*g/cc -27 GPa*g/cc)**,** Vp/Vs ratio (2.3-2.5), high acoustic impedance and low Mu-Rho indicated shale. The cross plot models all show similar result of hydrocarbon sand characterized by high porosity, low water saturation and volume of shale. The well based elastic attribute analyses established useful relationships between elastic derived seismic attributes and reservoir properties in delineating lithology and reservoir fluid for better understanding of reservoirs in the Niger Delta field.

Keywords: Reservoir characterization, elastic attributes. Reservoir properties, Reservoir fluid and lithology, cross-plots.

1. INTRODUCTION

Increasing exploration activities in the Niger Delta has focused attention toward improving qualitative and quantitative interpretation of the reservoir. Previous research have focused on the integration of well logs and seismic attributes to improve understanding of reservoir characteristics.Mis-interpretation of subtle features of reservoirs has resulted into bypass of hydrocarbon zones (Sheriff 1992). This makes their identification through several methodologies such as multi-dimensional attribute analysis and inversion difficult (Dvorkin et al., 2004; Avseth*et al.*, 2005; Adekanle and Enikanselu, 2013). However, elastic attribute has the capacity to properly discriminate lithology and fluid types of subtle features even beyond the drilled region. Well logs give estimates of reservoir properties like porosity, fluid saturation , shale content required for inversion. The three major logged elastic properties are: P-wave velocity, S-wave velocity and density. However, through petrophysical transforms other elastic properties such as acoustic impedance, V_P / Vs ratio, etc. could be generated from the log data. These elastic properties play an important role in reservoir characterization because they are related to the reservoir properties (Chi and Han, 2009). Whereas Rock physics is the bridge that links these elastic properties to the reservoir properties (Avseth*et al*., 2009; Dewar and Downton, 2002; Dvorkin *et al*., 2002; Miller, 1992; Carr *et al.,* 2002). Elastic attribute analyses rely on the empirical relations and different cross-plots shows these

derived elastic attributes are an indispensable tool for efficient interpretation of lithology and fluid of the target reservoir across the Niger delta field. (Ødegaard and Avseth, 2004; Omudu and Ebeniro, 2005; Mukerji and Mavko, 2006; Sayers and Boer, 2011). It useful for selecting different seismic elastic attributes, predict and calibrate different seismic response during interpretation (Avseth*et al*., 2005; Dvorkin *et al*., 2002; Pelletier *et al*., 2004). Significantly, different established derived elastics attribute trends help to characterize the reservoir further (Avseth*et al*., 2005; Ødegaard and Avseth, 2004).

2. BASIC THEORETICAL BACKGROUND

The basic seismic elastic waves that propagate through the earth are P and S waves velocities. These waves induce elastic deformation along the propagation path in the subsurface. P-wave can change the volume and shape of the unit rock while S-wave changes the shape of the unit rock. Relationship between P-wave **(**Vp**)** and S-wave **(**Vs**)** are commonly expressed as equations 1 and 2.

$$v_p = \sqrt{\frac{\lambda+2\mu}{\rho}} \quad Or \quad v_p = \sqrt{\frac{K+\frac{4\mu}{3}}{\rho}} \qquad \mathbf{1}$$

$$\lambda = K - \frac{2\mu}{3}$$

$$v_s = \sqrt{\frac{\mu}{\rho}} \qquad \mathbf{2}$$

$$Velocity\ ratio\ (\gamma) = \frac{v_p}{v_s} = \sqrt{\frac{\lambda+2\mu}{\mu}} \qquad 3$$

$$\text{Poisson ratio } (\sigma) = \frac{\gamma^2-2}{2\gamma^2-2} = \frac{\left(\frac{v_p}{v_s}\right)^2-2}{2\left(\frac{v_p}{v_s}\right)^2-2} \qquad 4$$

Poisson's ratio (σ) may be used to derived the relationship between

LambdaRho/MuRho$\left(\lambda\rho/\mu\rho\right)$ using the equation

$$\frac{\lambda\rho}{\mu\rho} = \frac{2\sigma}{1-2\sigma} \qquad 5$$

Hence, $$\sigma = \frac{\lambda\rho}{2\rho(\lambda+\mu)} \qquad 6$$

Where Vp = compressional wave velocity, Vs = shear wave velocity , λ = incompressibility sensitive to pore fluid, μ = rigidity modulus or shear modulus sensitive to rock matrix. Both ($\lambda\ and\ \mu$) are Lamé parameters, ρ = density K= Bulk modulus, Ip = P-Impedance, Is = S-Impedance,$\mu\rho$ = Lambda-Rho, $\lambda\rho$ =Mu-Rho.

Sensitivity of fluid and Lithology change can be determined from the velocity ratio between P-wave velocity and S-wave velocityrelations derived from seismic or sonic log data (Castagna et al., 1993, Ogungbemi, 2014). P-wave velocity travel through both fluid and rock but more sensitive to fluid changes than S- wave velocity. Hence changes in velocity ratio ($\frac{v_p}{v_s}$) can indicate fluid saturation within the reservoir. Castagna et al. (1985) proposed different velocity ratio for different lithologies as shown in table 1

Table 1: Different rock types Velocity ratio proposed by (Castagna et al., 1985).

Rock type	velocity ratio $\left(\frac{v_p}{v_s}\right)$ range
Fine grained sand	1.1 - 1.2
Medium grained sand	1.2 – 1.45
Coarse grained sand	1.46 – 1.6
Sandstone	1.6 - 1.8
Shale or clay	>2.0

The Vp/Vs ratio, however, is not dependent of density and can be used to derive Poisson's ratio, which is a considerably more diagnostic lithology indicator (Kearey*et al.,* 2002). For different lithologies of the same fluid, normally the shalier lithology will plot at relatively higher Poisson`s ratio than the sand lithology. Poisson's and velocity ratios aid in fluid and lithology discrimination.
However, velocity ratio may not be effective in delineating carbonate lithology (Clement, 2015**)**. Lithology prediction using Lamé parameter detect these short fall of lithology separation using velocities. Several authors have established and determined reservoir properties utilizing Lamé parameter to gain understanding into rock physics (Goodway, 2001; Dewar and Downton 2002; Perez and Ton, 2010). Lambda-rho (λρ) or Incompressibility is determine from the square difference of acoustic impedance and shear impedance as expressed in equation 4. It is a basic property that is more obvious in its association and increasingly evident relationship to reservoir properties when compared to the usual seismic attributes like amplitude use for reservoir fluid indicator (Gray and Anderson, 2000). Lambda-rho can be useful for pore fluid detection and lithology discrimination. Low Incompressibility values are related with gas sand (Goodway *et al*., 1997). . Research has indicated that water saturated sandstone have higher density than hydrocarbon saturated sandstone (Klein and Philpotts, 2012). Consequently, hydrocarbon saturated sandstone have low Lambda-rho values. Mu-rho (μρ) referred to as rigidity is sensitive to rock's matrix and not affected by fluid. It is useful for lithology discrimination. High rigidity values are associated with sands while low values indicate shales (Goodway *et al*., 1997). High rigidity of sandstone due the dominant mineralogy (quartz) as compared to the feldspar content of shale or clay. According to (Gidlow *et al*, 1992) the expressed by the P and S impedance contrasts is more accurate than those expressed by other pairs of contrasts of elastic parameters, such as lambda and mu. Although the *lambda* and *mu* can be obtained from the seismic inversion (Gray, 2002), the products of the lambda and density or mu and density can be transformed from the P and S impedances. Petrophysical inversion of these rock impedances for rock-fluid properties given a reservoir relationship between the acoustic properties and rock-fluid properties (Doyen, 1988). Cross plot of these parameters also aid in lithology and fluid discrimination, which is the main objectives of this research, hence the need to analyze these parameters.

3. THE STUDY LOCATION AND GEOLOGY

The study area (Figure 1) is located in the southeastern part of Niger Delta. The Niger delta is a sedimentary depression of significant Cenozoïc deltaic formation in the Gulf of Guinea. The present-day Niger delta is believed to be laid on oceanic crust whose deltaic sediments reflect upward transition from marine pro-delta shales (Akata Formation) through a deltaic paralic interval (Agbada Formation) to a continental sequence (Benin Formation) deposited in fluvial environments (Weber and Daukoru, 1975;

Weber 1987). Oil and gas in the Niger Delta are mainly trapped in sandstones and unconsolidated sands in the Agbada formation. The steady progradation of the Niger Delta Basin has been accompanied by the development of growth faults, associated with rollover anticlines and mud diapirism (Busting, 1988, Doust and Omatsola,1989). This has resulted to a series of strike-parallel, fault-bound depositional belts which show successive younging from north to south. Oil and gas are mainly trapped by rollover anticlines and fault closures.

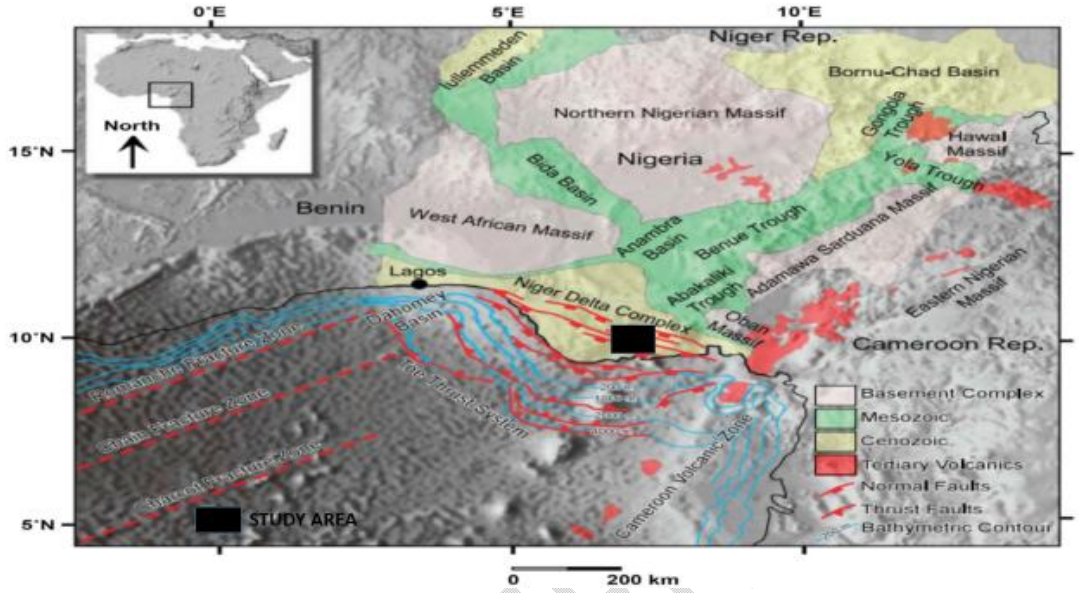

Figure 1: The Location of the study area within the Niger Delta region

4. MATERIALS AND METHOD

The Field well data comprises of three wells with the available petrophysical logs (P-wave, density, gamma and resistivity) utilized in this study (Figure 2). The wells were displayed in TVD (True vertical depth) in feet. The Hampson-Russell Software (10.0 version) was used for interpretation analysis with the work flow (Figure 3) adopted for this study. Firstly Log (ASCII Standard) files were reviewed for curve availability, the Kelly bushing elevation and logs identification. Well logs were quality check for abnormal and spurious event. Qualitative interpretation was done by combination of gamma ray and resistivity logs in picking the sand tops at the zone of interest. Sand B20 was delineated based on low gamma ray counts and high electrical resistivity values. Petrophysical parameter was quantitatively estimated using some empirical equations for shale volume calculation, porosity, permeability and fluid saturation determinations in the reservoir zone. Due to absence of S-wave (Vs) data, the empirical relation of Greenberg-Castagna was used to prediction Vs from Vp (Castagna et al.,1993). The sonic Vp, density log (RHOB) and estimated Vs were used to generate P-impedance and S-impedance values at each well, other elastic properties such as Lambda Rho (λρ), MuRho (μρ), Vp/Vs Ratio , Poisson ratio, were derived using empirical relationships between them and the available parameters . Cross plotting of these elastic properties was carried out, colour coding with reservoir properties likePorosity, Water saturation (Sw), and Shale volume (Vsh) (in the z-component axis). This further reveals the relationships between various elastic and reservoir properties of the target reservoir.

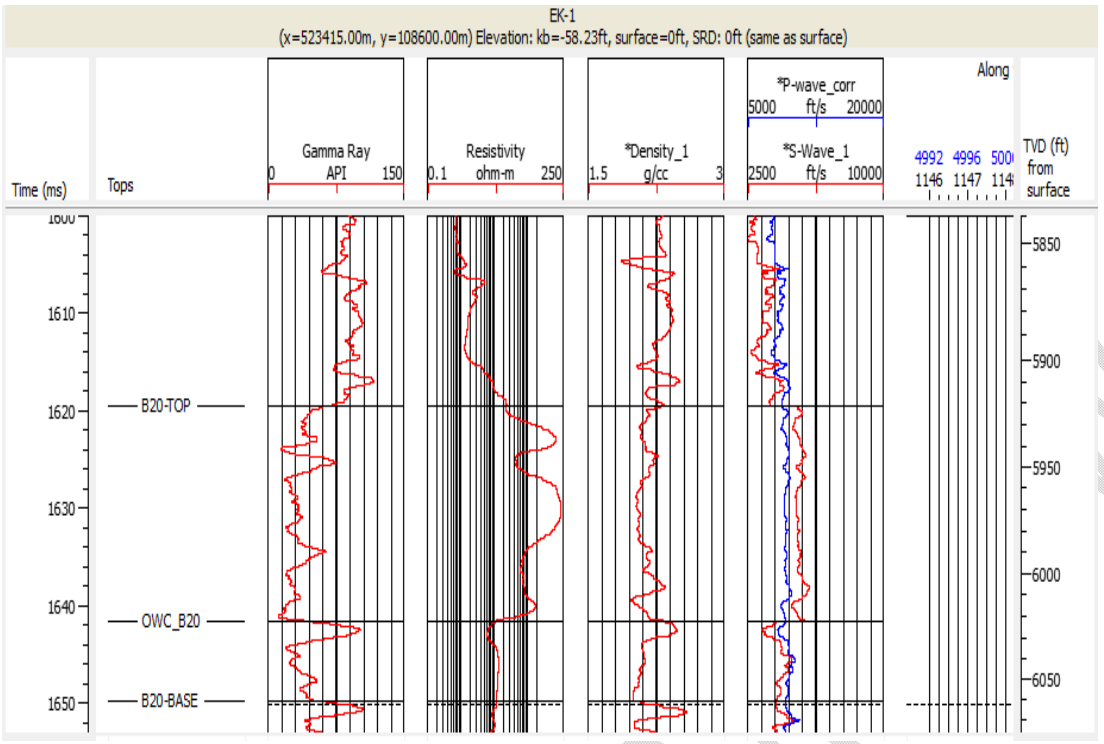

Figure 2: Wireline logs used for the study

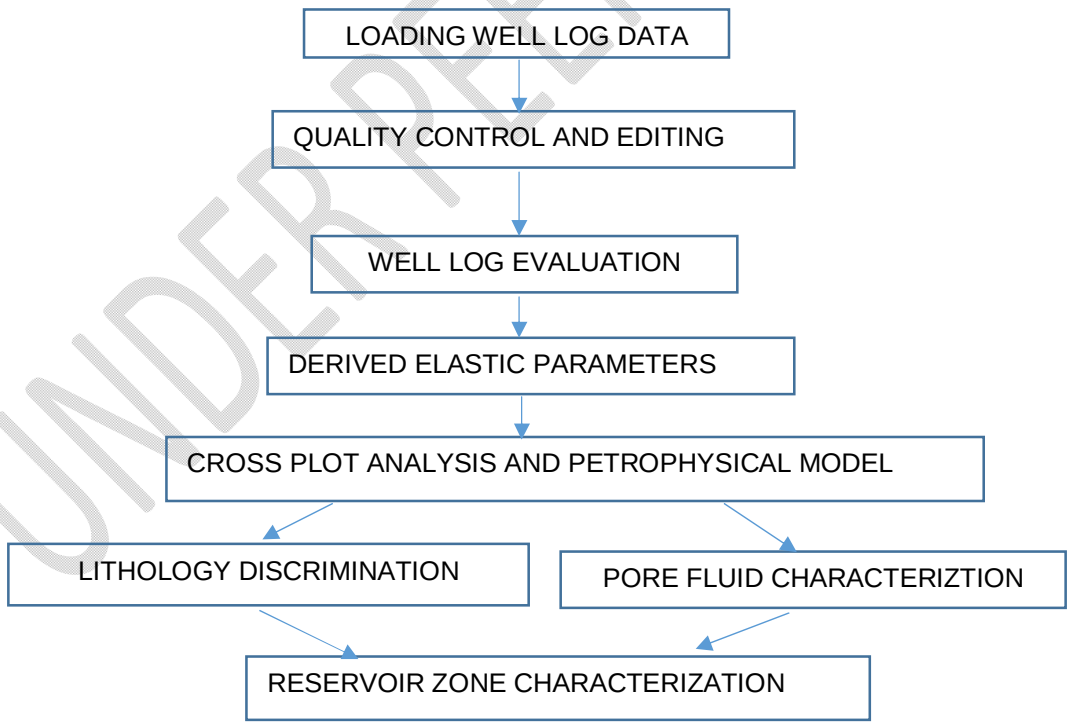

Figure 3: Work flow chart

5. PRESENTATION OF RESULT

The hydrocarbon bearing reservoir sand B20 at 5860 ft – 6106ft in the wells was delineated based on low gamma ray counts and high electrical resistivity values (Figure 2).Petrophysical parameters within this reservoir is estimated to have average porosity and effective porosity value of 33.92% and 33.92% respectively. Average water saturation of 24.41% indicates 75.59% hydrocarbon saturation. The sands are well sorted with low values of the Vshale with an average value of 7.50%.

Table 2.Petrophysical parameters measured in the reservoir

Wells	**Depth (ft)**	**Thickness** (ft)	**POROT (%)**	**VSH (%)**	**POROE (%)**	**K (mD)**	**Sw (%)**
Wells EK1 B20 Top-B20 Base	5860 -5965	105	31.20	7.65	28.93	1362.98	27.50
Well EK2 B20 Top-B20 Base	5796-5934	138	38.39	8.69	28.47	1720.67	19.92
Well EK3 B20 Top-B20 Base	5990-6106	116	32.19	6.18	30.30	1477.34	25.82
Average		120	33.92	7.50	29.23	1337.66	24.41

The following parameter cross plots were made;
1. Mu-Rho versus Lambda-Rho
2. Vp/Vs ratio versus Lambda-Rho
3. Poisson's ratio versus Lambda-Rho
4. Acoustic Impedance versus Vp/Vs
5. Poisson's ratio versus Vp/Vs

Cross plot Model of Mu-rho versus Lambda-rho

The cross plot of Mu-Rho vs Lambda-Rho colour coded with volume of shale is shown in Figure 4a. The separation of hydrocarbon sands (blue ellipse) with low Lambda-Rho (7-10) GPa*g/cc from brine sand (red ellipse) value of about (17-21) GPa*g/cc and shale (black ellipse) with high Lambda Rho (24-27) GPa*g/cc values shows a good litho-fluid discriminator in this field. Low Mu-Rho correspond to high shale volume and high Mu-Rho clearly indicate hydrocarbon sand. The anomalous data point (hydrocarbon sand) indicate high porosity, low water saturation when cross plot of Mu-rho vs Lambda-rho is colour coded by these reservoir properties on the z-axis as seen in (Figure 4(b-c)) respectively.

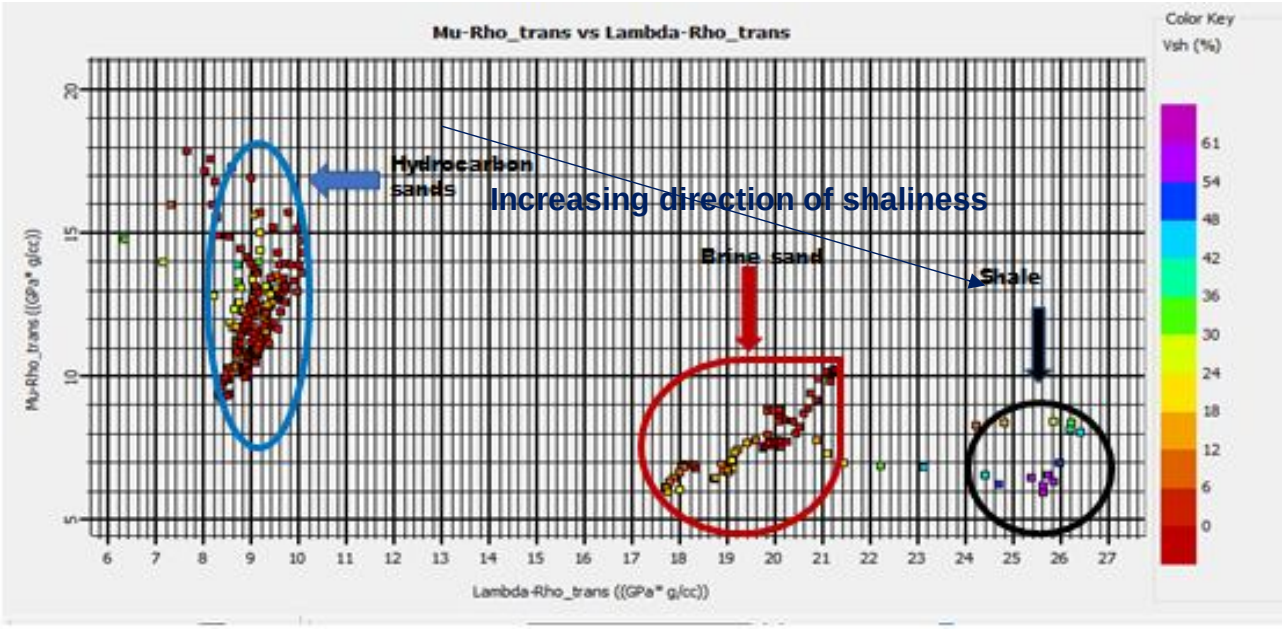

Figure 4a: Cross-plots of Mu-Rho vs Lambda-Rho colour coded with shale volume

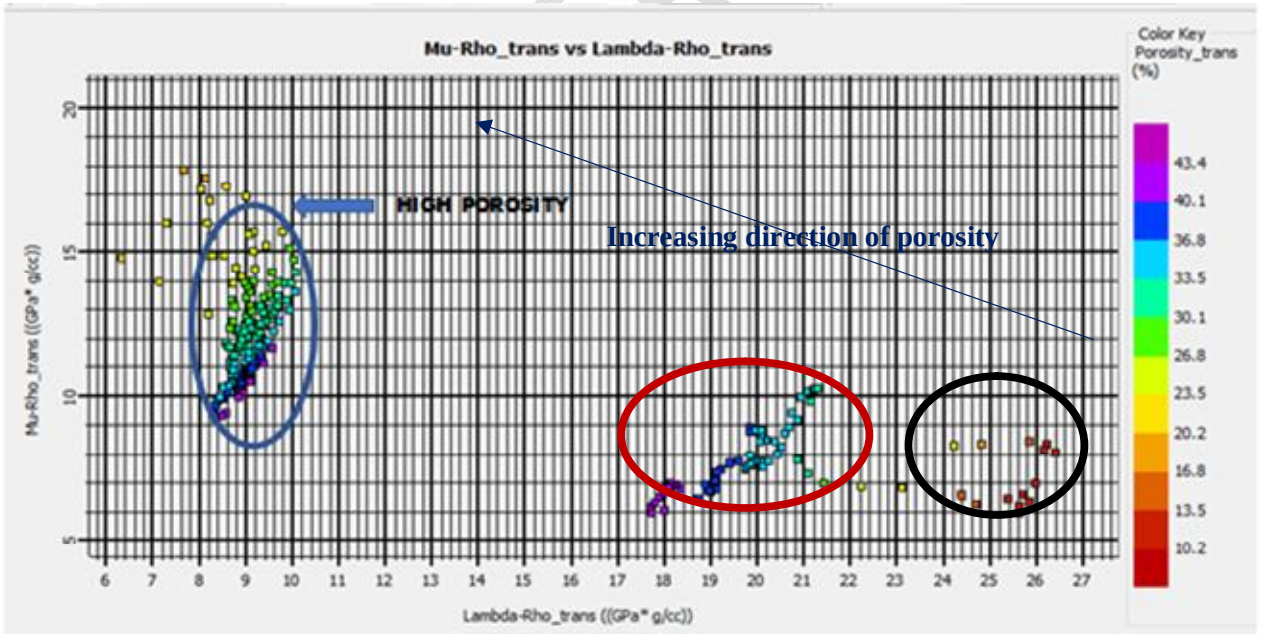

Figure 4b: Cross-plots of Mu-Rho vs Lambda-Rho colour coded with porosity

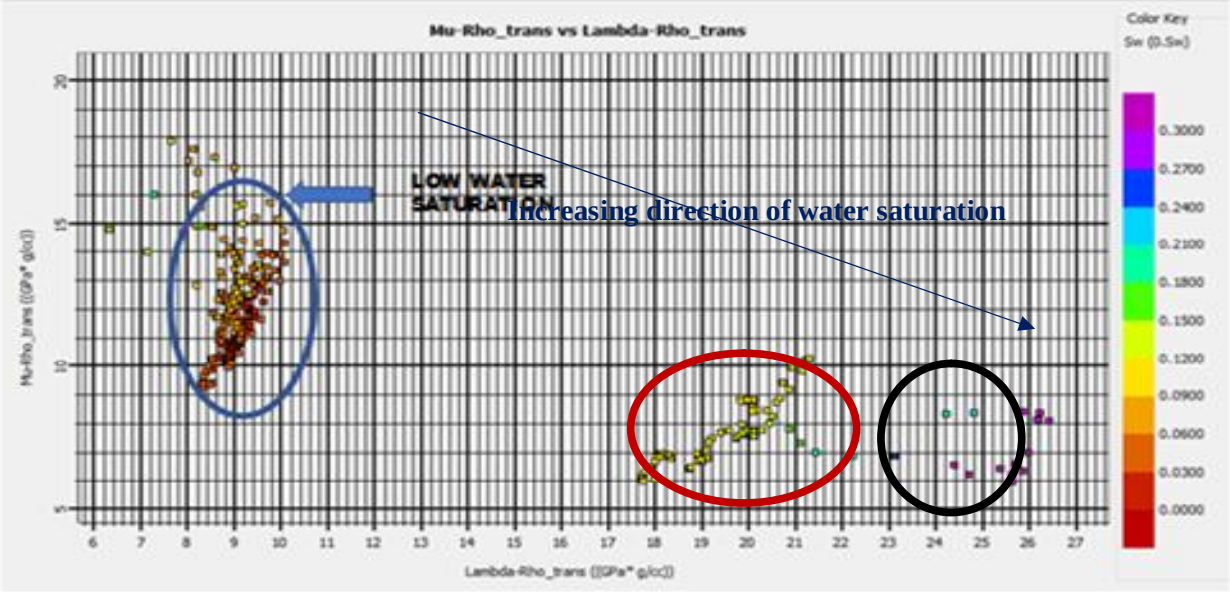

Figure 4c: Cross-plots of Mu-Rho vs Lambda-Rho colour coded with water saturation

Cross-plots of Vp/Vs ratio versus Lambda-rho

Changes in Vp/Vs ratio and Lambda-Rho are fluid indicator as displayed in cross-plots of Vp/Vs vs Lambda-Rho colour coded with porosity on the z-axis (Figure 5a). This shows the hydrocarbon sand (blue ellipse) is characterize by low Lambda-rho and low Vp/Vs ratio of (1.6-1.8) value range while brine sand (red ellipse) shows Vp/Vs ratio (2.05-2.3) and shale (black ellipse) has high Vp/Vs ratio of (2.3-2.5) with corresponding high Lambda-Rho value. Porosity, Volume of shale and Water saturation attributes plotted on the z-axis showed distinguish trend of increasing direction which is useful in establishing relation between the Hydrocarbon sand, brine sand zone and shale zone. The hydrocarbon sand indicated low shale volume, low water saturation as seen in the cross plot of Mu-rho vs Lambda-Rho colour coded by these reservoir properties on the z-axis (Figure 5(b-c)).

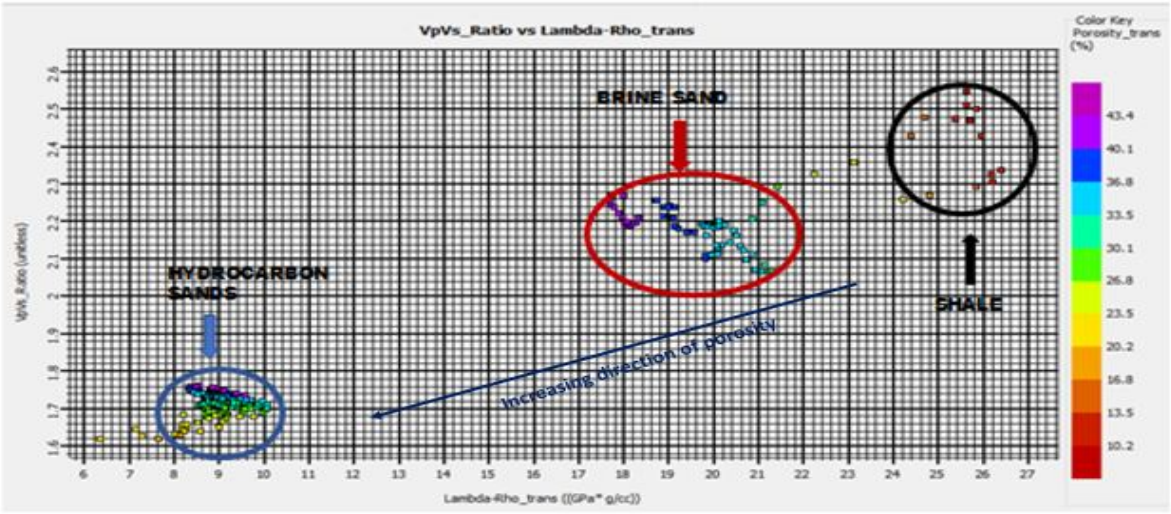

Figure 5a: Cross-plots of Vp/Vs ratio vs Lambda-Rho colour coded with porosity

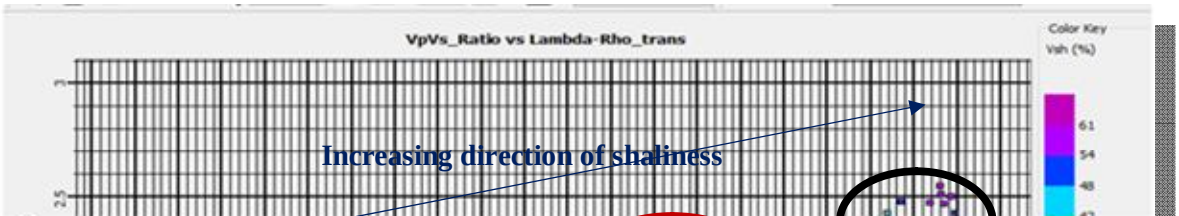

Figure 5b: Cross-plots of Vp/Vs ratio vs Lambda-Rho color coded with Vshale

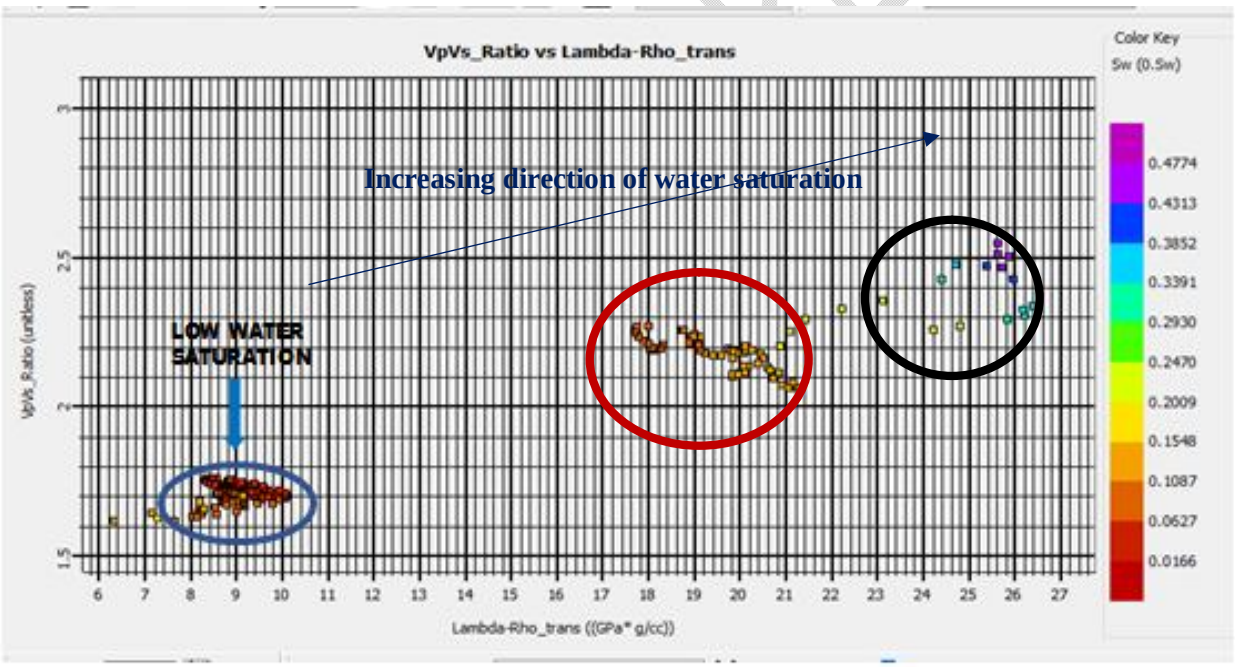

Figure 5c: Cross-plots of Vp/Vs ratio vs Lambda-Rho color coded with water saturation

Crossplot of Poisson's ratio versus Lambda-Rho The crossplot of Poisson's ratio vs Lambda-rho colored coded by Vshale (Figure 6a) shows of hydrocarbon saturated sands (blue ellipse) with relatively low Poisson's ratio (0.2-0.26) compared to surrounding shaly

lithology (red & black ellipse) with overlapping higher Poisson's ratio of (0.35-0.41). This anomalous data points (hydrocarbon sand) indicated high porosity, low water saturation when cross plot of Poisson's ratio and Lambda-Rho colour coded by these reservoir properties as seen in (Figure 6 (b-c)) respectively.

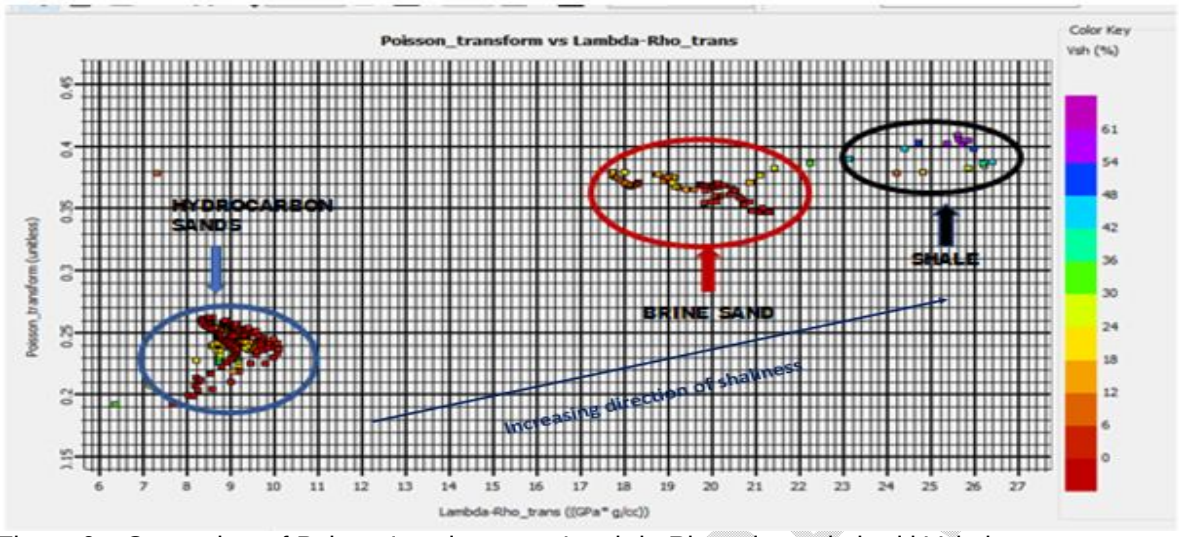

Figure 6a: Cross-plots of Poisson's ratio versus Lambda-Rho color coded withVshale

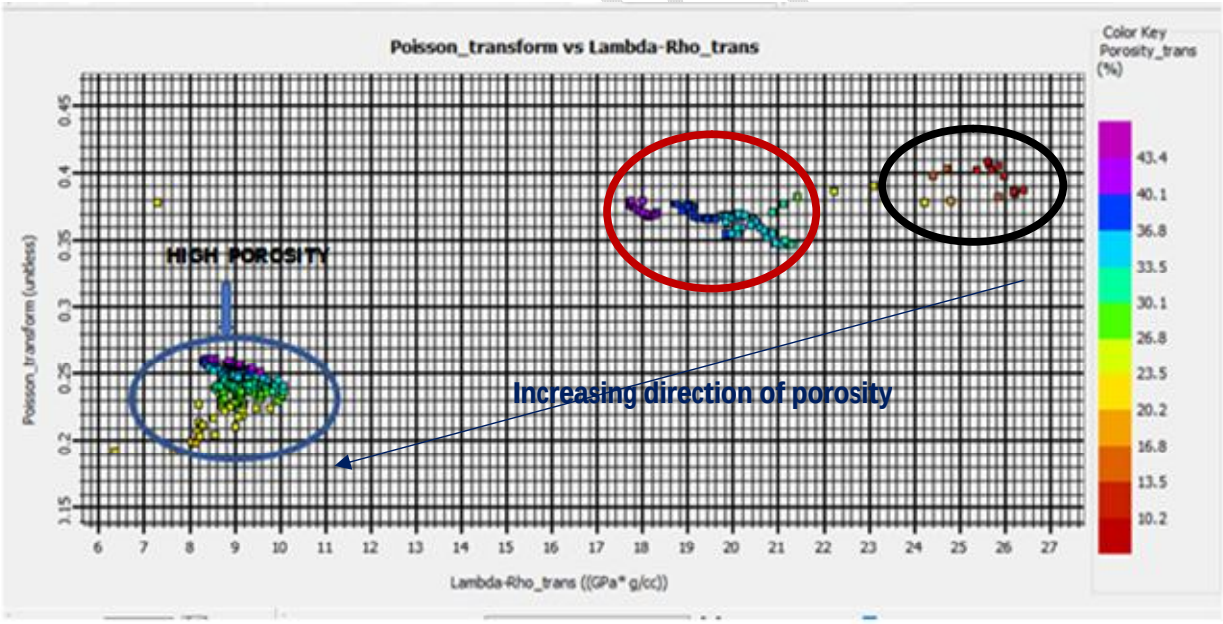

Figure 6b: Cross-plots of Poisson's ratio vs Lambda-Rho color coded with porosity

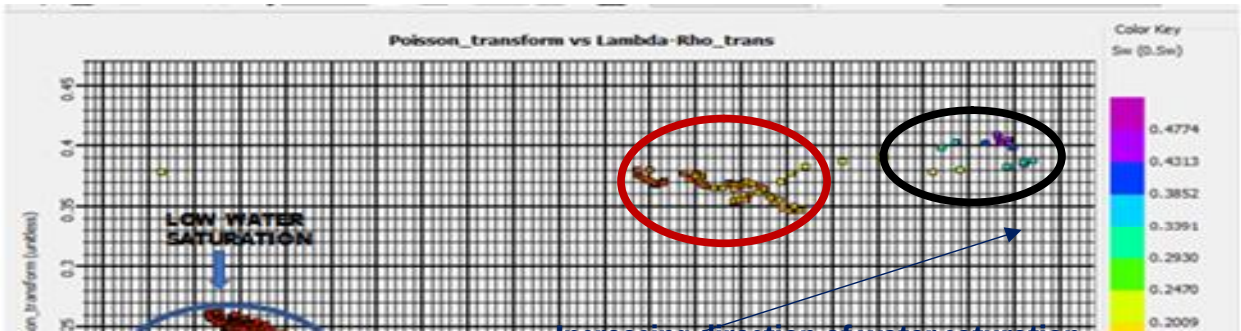

Figure 6c: Cross-plots of Poisson's ratio vs Lambda-Rho color coded with water saturation

Crossplot of acoustic impedance versus Vp/Vs

Changes in the fluid type result in changes in Vp/Vs ratio, as displayed in cross-plots of Vp/Vs vs acoustic impedance colour coded with volume of shale (Figure 7a). This shows the hydrocarbon sand (blue) is characterize by lowVp/Vs ratio and acoustic impedance while both brine sand (red) and shale (black) has high Vp/Vs ratio and acoustic impedance . The hydrocarbon sand indicated low shale volume, low water saturation, and high porosity as seen in the cross plot acoustic impedance against Vp/Vs colour coded by these reservoir properties (Figure 7 (b-c). Porosity, Volume of shale and Water saturation attributes plotted on the z-axis showed distinguish trend of increasing direction which is useful in establishing relation between the Hydrocarbon sand, brine sand zone and shale zone. Shaliness and water saturation increasing from west to east, peaking at the shale zone (Figure 7a and Figure 7b) while porosity trend increasing from east to west, peaking at the hydrocarbon sand (Figure 7c).

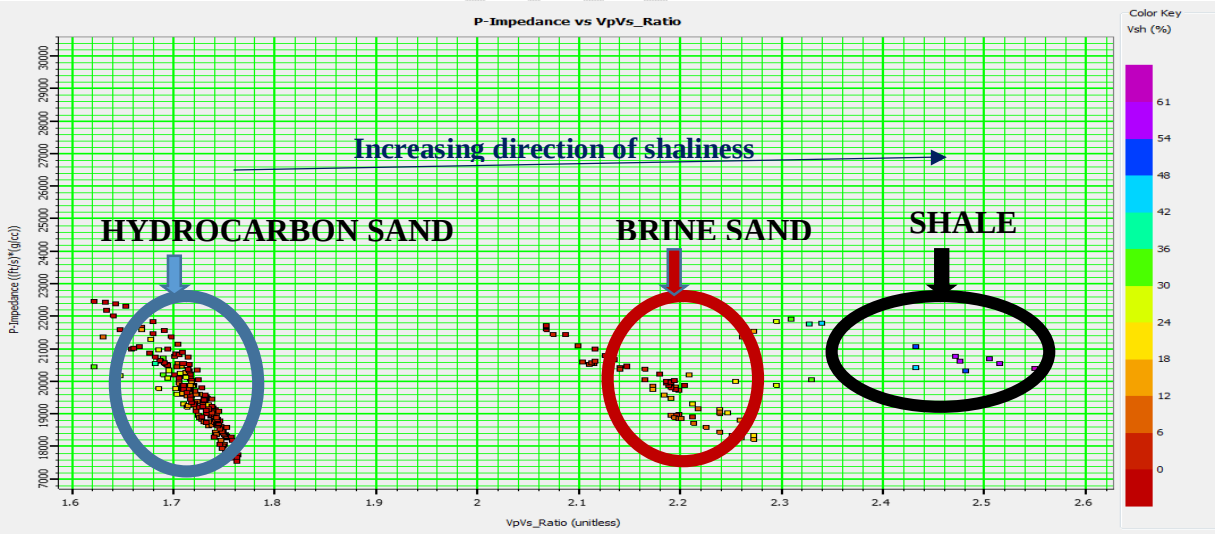

Figure 7a: Cross-plots of acoustic impedance vs Vp/Vs ratio colour coded with volume of shale

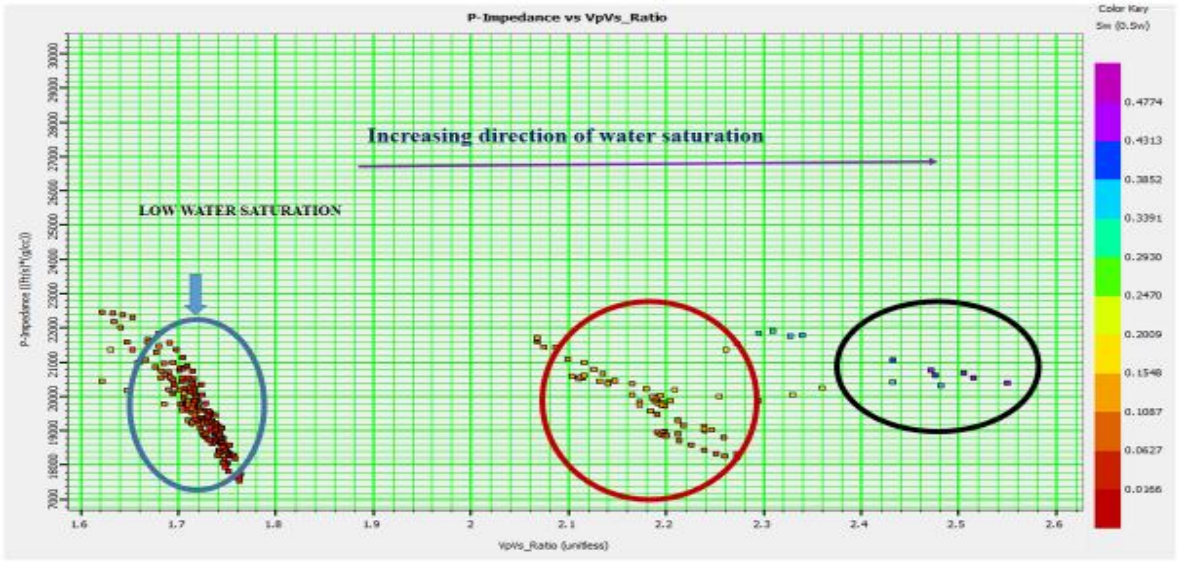

Figure 7b: Cross-plots of acoustic impedance vs Vp/Vs ratio colour coded with water saturation

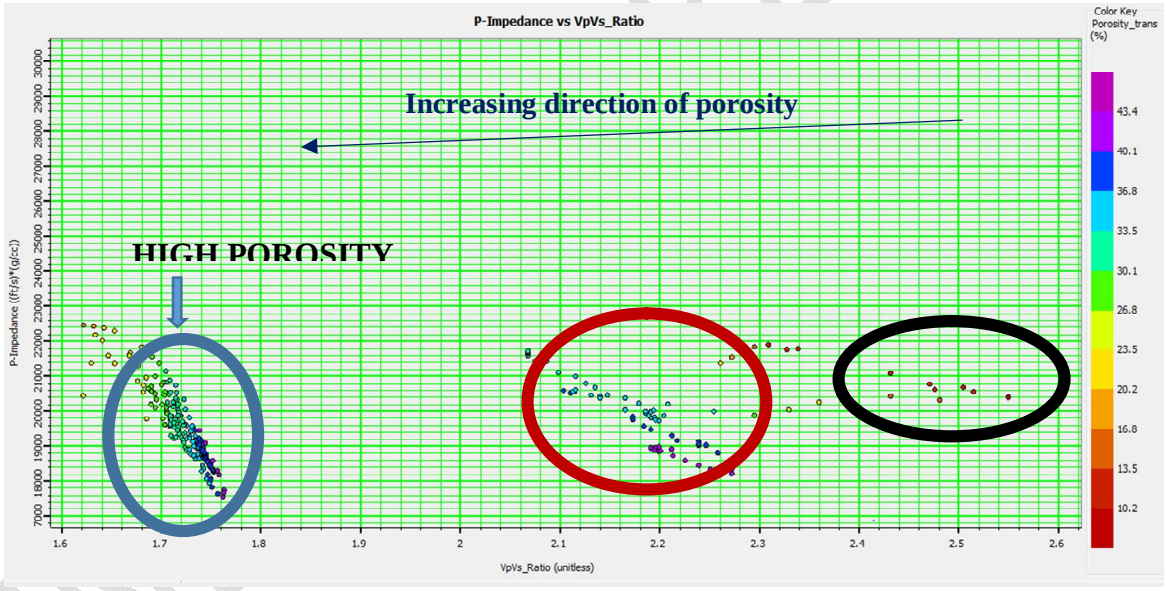

Figure 7c: Cross-plots of acoustic impedance vs Vp/Vs ratio colour coded with porosity

Crossplot of Poisson's ratio versus Vp/Vs

The crossplot of Poisson's ratio versus velocity ratio colour coded with Lambda-Rho, volume of shale, depth,water saturation plotted on the Z-axis, identified pore fluid content and associated lithology (Figure 8(a-d)). The gas sand, oil sand, brine sand, and shale was selected on the crossplot based on the interpretation guideline (figure 1). The selected area in blue zone represents hydrocarbon sand characterized with low Poisson`s and Vp/Vs ratios. The red and black selected area represents the brine sand and shale. Crossplot of Poisson vs Velocity ratio with Lamda Rho and Volume of shale on z-axis (Figure 8a, 8b) was effectively use to delineate fluid and lithology. When depth was ploted on the z- axis (figure 8c), it was observed the hydrocarbon sand occupy the shallow depth, follow by shale lithology and sand brine at the deepest depth .

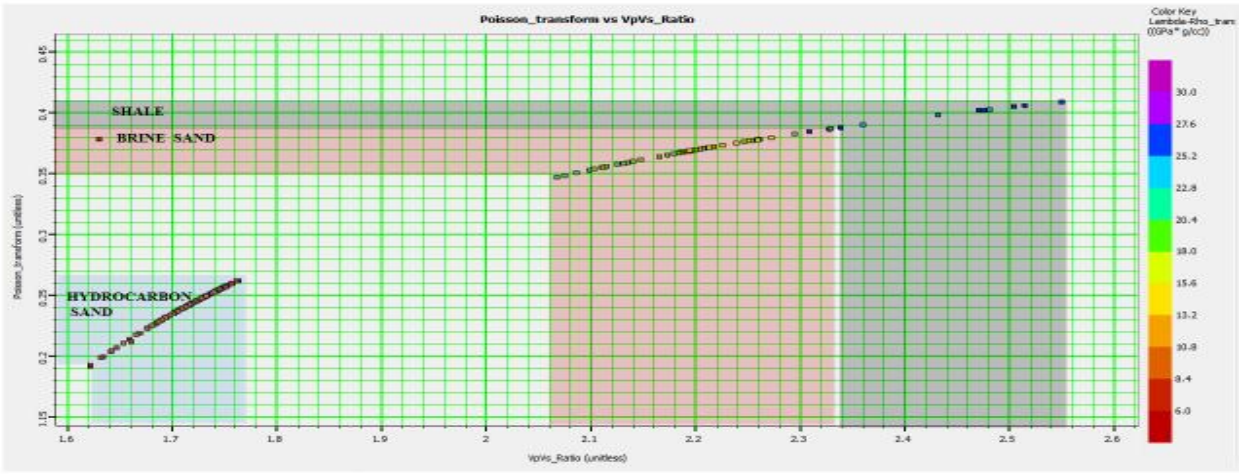

Figure 8a: Crossplot of Poisson's ratio vs. Vp/Vs colour coded with Lambda Rho

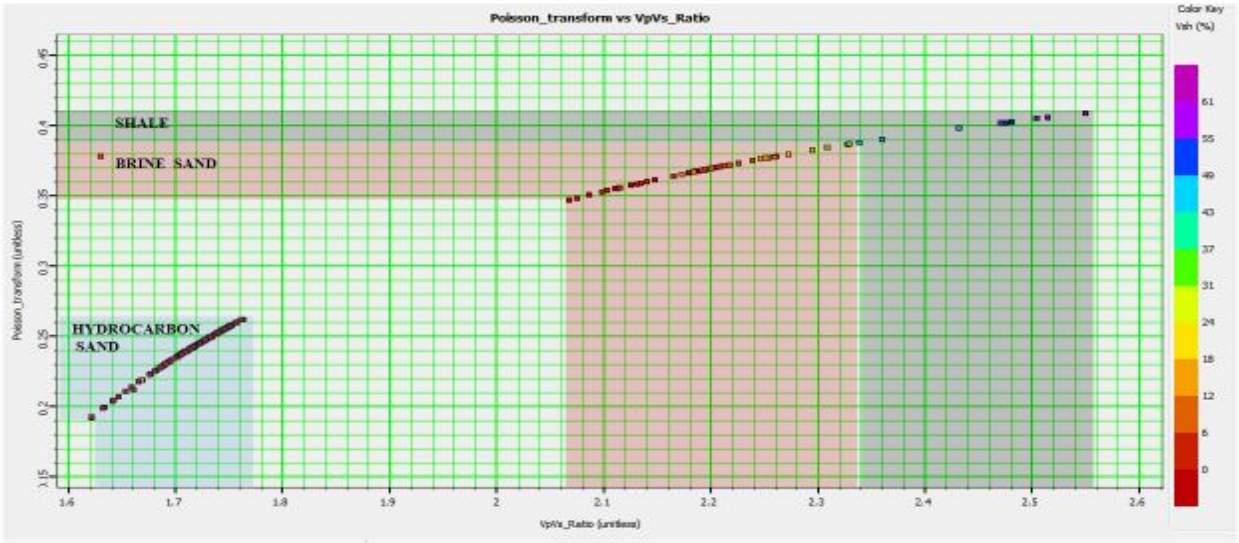

Figure 8b: Crossplot of Poisson's ratio vs. Vp/Vs colour coded with volume of shale

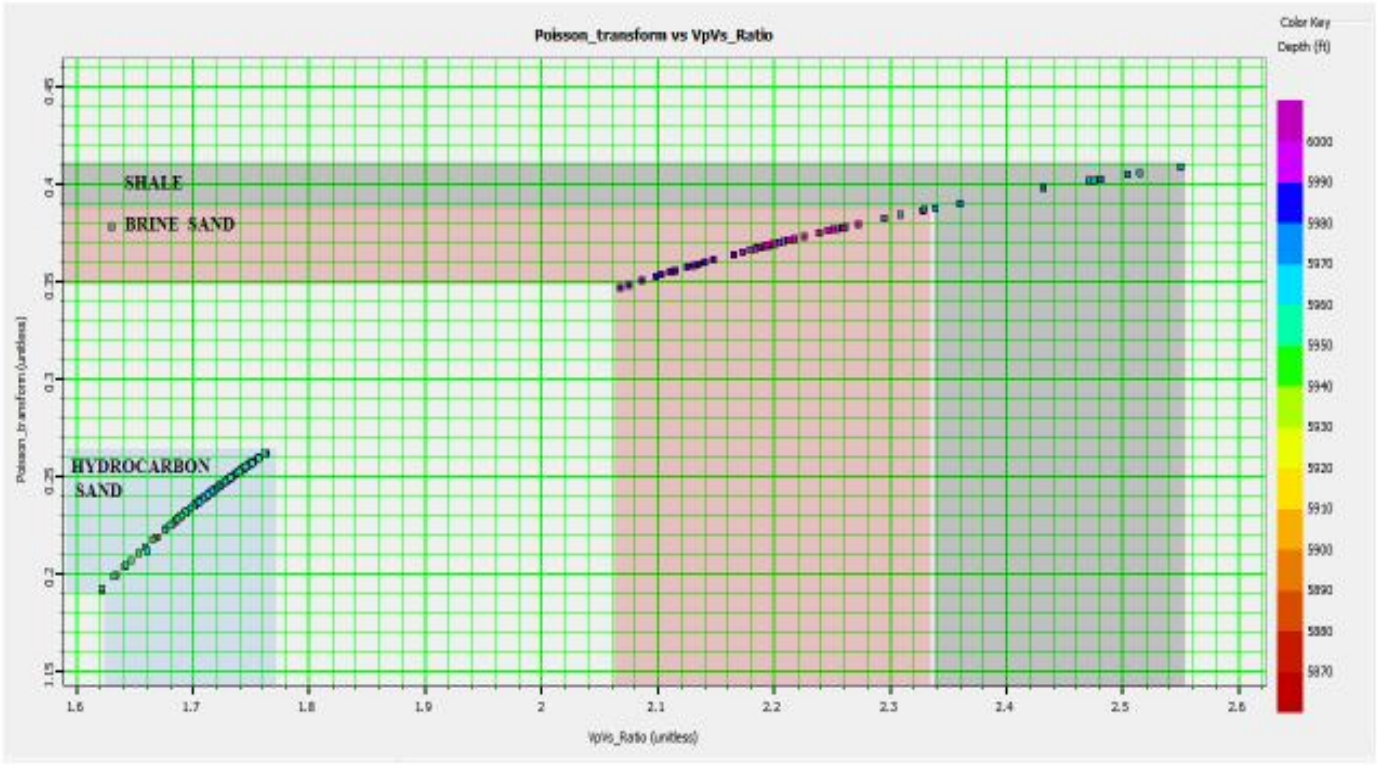

Figure 8c: Crossplot of Poisson's ratio vs. Vp/Vs colour coded with depth

6. DISCUSSION OF RESULT

The various cross-plots analysis of Mu-Rho versus Lambda-Rho, Vp/Vs versus Lambda-Rho , Poisson ratio versus Lambda-Rho, Acoustic Impedance versus Vp/Vs, Poisson's ratio vs. Vp/Vs with reservoir properties (porosity, volume of shale , water saturation and depth) on the z-axis shows good discriminative capacity for reservoir B20 fluids and lithology. The cross plot of Mu-Rho versus Lambda-Rho accurately defined litho-fluid character within reservoir B20 intervals that could be utilized for further rock property analysis. The Mu-rho attribute described the variation in rigidity which is related to the rock matrix and hence, lithology. High Mu-Rho (rigidity) as seen in the crossplot is associated with sandstone due to the dominant mineral of quartz in the sand than shale with low value. The Lambda-rho attribute infers the incompressibility moduli of the fluid content. The density of hydrocarbon saturated sandstone is less than brine sandstone. Hence, the hydrocarbon charged zones have a lower Lambda-rho values when compared to the brine sand. The shale within the reservoir has the highest Lambda-Rho values.

Lithology and fluid content are identified using Cross-plots of Lambda Rho versus Vp/Vs Ratio prove Lambda rho being a better tool in separating shale from brine and hydrocarbon zones. Most of the data points fall on the hydrocarbons saturated and water saturated sandstone zone. The hydrocarbon sand zones are captured in the cross plot corresponds to a low a value of Vp/Vs . Velocity ratio decreases in hydrocarbon layers because bulk modulus decreases in compressional wave velocity while shear wavevelocity increases in an oil layer, (Bahremandi*et al.,* 2012) Hence, velocity ratio is more sensitive to fluid change than individual Vp and Vs (Ødegaard and Avest, 2004; Rider and Kennedy, 2011).

The Crossplot of acoustic impedance versus Vp/Vs shows the hydrocarbon-saturated sand reservoir was characterized by a reduction in acoustic impedance as compared to the surrounding non-reservoir area

(shale and shaly sand). The attributes VP/VS appear to be more sensitive to fluid changes than the acoustic impedance. Lambda (λρ) has been identified in this study to be a better litho-fluid discriminator when compared with other seismic attributes because it contains bulk density which has assisted in defining the lithology and fluid types properly.
The biggest advantage of crossplotVp/Vs vs Poisson ratio crossplotcolour coded with Lambda Rho, volume of shale and depth is that it delineate vertical variations of hydrocarbon sandstone, shale and brine sandstone zone of reservoir B20 in that order. Hence, Poisson's ratio is a good fluid discriminator in this field which agreed with the interpretation guide adopted from Avseth Per lecture note. (Avseth*et al.,* 2005).

Summarily, Low Poisson's ratio, lambda-rho, Vp/Vs, acoustic impedance and high mu-rho indicate hydrocarbon sands. The intermediate values of this rock attributes indicated brine sand while high Poisson's ratio, lambda-rho, Vp/Vs, acoustic impedance and low mu-rho indicated shale. The cross plot models all shows similar result of hydrocarbon sand characterized by high porosity, low saturation, high resistivity and low volume of shale. Asides the notable separation observed in discriminating the hydrocarbon bearing sand from neighboring brine sand and shale, these reservoir properties highlighted trends and reaffirmed the occurrence of hydrocarbon bearing sands (blue ellipse), brine sand (red ellipse) and shale (black ellipse) with their diagnostic fluid and lithology discriminating potentials. Consequently, this gave more credence to our interpretation.

7. CONCLUSIONS

The results obtained demonstrate that the derived elastic attributes in relation to reservoir properties was successfully used in characterisation of reservoir B20 zones. The cross plot models shows useful established relationship between elastic attributes and reservoir properties. The Cross-plots attributes of Lambda- Mu-Rho ,Vp/Vs, , Poisson's ratio and acoustic impedance were good tools utilized for litho-fluid prediction within the reservoirs. Prediction of the variation of lithological and fluid reservoir properties such as porosity, volume of shale, water saturation and depth throughout the reservoir volumes is important for exploration and developmentof hydrocarbon reservoirs. The Cross plotting and reservoir models provide new method to predict the sandstone reservoir distribution, reservoir quality, and fluid content potential. Hence this study serve as a practical pre-step to quantitative reservoircharacterization from seismic data which aid in reduction of uncertainties and essential for reservoir development and production enhancement.

REFERENCES

1. Chi, X.G., Han, D.H. (2009). Lithology and fluid differentiation using a rock physics template. Leading edge, 1424 – 1428
2. Avseth, P., Jørstad, A., Van wijngaarden, A. J. and Mavko, G. (2009). Rock physics estimation of cement volume, sorting, and net-to-gross in North Sea sandstones. *The Leading Edge,* 28**,** 98-108.
3. Dewar, J., Downton J. (2002). Getting unlost and staying found – a practical framework for interpreting elastic parameters. Expanded Abstract CSEG Annual Conference 2002.
4. Dvorkin Jack, Carr Matthew B., and Berge Tim (2002) "Rock Physics Diagnostic in Sand/Shale Sequence." EAGE 64th Conference and Exhibition Florence, Italy, 27.
5. Miller Susan L. M. (1992) "Well Log Analysis of Vp and Vs in Carbonates." CREWES Research Report 4.
6. Carr Matthew B., Hubert Lars, and Dvorkin Jack (2002) "Shear Velocity Prediction in the Norwegian Sea." EAGE 64th Conference and Exhibition Florence, Italy.
7. Dvorkin Jack, Fasnacht Timothy, Uden Richard (2004) "Rock Physics for Fluid and Porosity Mapping in Ne Gom." no. EAGE.

8. Ødegaard, E., Avseth, P. (2004). Well log and seismic data analysis using rock physics templates.
9. Omudu L. M. and Ebeniro J.O. (2005) "Cross-Plotting of Rock Properties for Fluid Discrimination Using Well Data in Offshore Niger Delta." Nigerian Journal of Physics, 17.
10. Mukerji Tapan and Gary Mavko (2006) "Recent Advances in Rock Physics and Fluid Substitution." CSEG Recorder, Special Edition.
11. Sayers Colin M., And Lennert D. Den Boer (2011) "Rock Physics-Based Relations for Density and S-Velocity Versus, P-Velocity in Deepwater Subsalt Gulf of Mexico Shales." The Leading Edge Physics of rocks.
12. Gassmann F., (1951) Uber die elastizitat poroser medien. Vier. Natur Gesellschaft, 96, 1-23.
13. Avseth Per, (2010) Exploration Rock Physics the Link between Geological Processes and Geophysical Observables (Chapter 18), Petroleum Geoscience by Bjørlykke K.: From Sedimentary Environments to Rock Physics." Pp 403-426.
14. Avseth Per, Mukerji T.andMavko G. (2005). Quantitative Seismic Interpretation: Applying Rock Physics Tools to Reduce Interpretation Risk. Cambridge, Cambridge University Press.
15. Pelletier Heath Jay Gunderson, Veritas DGC (2004) "Application of Rock Physics to an Exploration Play: A Case Study from the Brazeau River 3d." CSEG National Convention Great Explorations – Canada and Beyond.
16. Avseth Per, Mukerji, T., Jorstad, A., Mavko, G. and Veggeland, T (2001) "Seismic Reservoir Mapping from 3-D Avo in a North Sea Turbidite System." Geophysics, Soc. of Expl. Geophys, 1157-1176.
17. Walls Joel, Dvorkin Jack, Carr Matt (2004) "Well Logs and Rock Physics in Seismic Reservoir Characterization." Rock Solid Images Offshore Technology Conference.
18. Alexander, T., J. Baihly, C. Boyer, B. Clark, G. Waters, V. Jochen, J. Calvez, R. Lewis, C. Miller, J. Thaeler, and B. Toelle “Shale Gas Revolution.” Oilfield Review (2011).
19. David C. and Ravalec-Dupin, Le M. (2007) "Rock Physics and Geomechanics in the Study of Reservoirs and Repositories." Geological Society, London, Special Publications 2007, v.284, 1-14.
20. Ostrander, W. J. (1984). Plane-wave reflection coefficients for gas sands at normal angle of incidence. Geophysics, 49(10), 1637-1649.
21. Castagna, J. P., Batzle M. L. and Kan T. K. (1993). Rock physics - The link between rock properties and AVO response, in offset-dependent reflectivity - Theory and practice of AVO analysis, ed. J. P. Castagna and M. Backus. Investigation in Geophysics, No. 8, SEG, Tulsa, Oklahoma, p. 135-171.
22. Ogungbemi, O.S. (2014). Prediction of Lithology Using the Ratios of Compressional and Shear Wave Velocities and their Travel Times. Pacific Journal of Science and Technology. Vol. 15. pp. 355- 359.
23. Castagna, J.P., Batzle, M.L., Eastwood, R.L. (1985). "Relationships between compressional wave and shear wave Velocities in Clastic Silicate Rocks". Geophysics. 50(4): pp. 571-581.
24. Kearey, P., Brooks, M., Hill, I. (2002). An Introduction to Geophysical Exploration. 3rd Edition. Blackwell Science: Oxford, UK. 236 - 262.
25. Clement Obeng-manu, (2015). Lithology and pore fluid prediction of a reservoir using density, compressional and shear wave logs. A thesis submitted to the department of physics, Kwame Nkrumah University of Science and Technology, Kumasi.
26. Goodway, W. (2001). AVO and Lame’ constants for rock parameterization and fluid detection. pp. 39-60.
27. Perez, M.A., Tonn, R. (2010). Reservoir modelling and interpretation with Lamé’s parameters: A Grand Banks Case Study.
28. Gray, F. David and Eric C. Andersen (2000) "Case Histories: Inversion for Rock Properties." EAGE 62nd Conference and Technical Exhibition, Glasgow, Scotland.
29. Goodway Bill., Taiwen. Chen. and Downton Jon. (1997) "Improved Avo Fluid Detection and Lithology Discrimination Using Lamepetrophysicalparameters: From P and S Inversions." The Leading Edge, Extended Abstracts, Soc. Expl. Geophysics 67, 128-138.
30. Klein, C. and Philpotts, A. (2012). Earth Materials: Introduction to Mineralogy and Petrology. pp. 361 – 362.
31. Gidlow,P.M.,Smith, G.C.,and Vail, ,P.J., (1992). Hydrocarbon detection using fluid factor traces, a case study: How useful is AVO analysis? Joint SEG/EAEG summer research workshop, Technical Program and Abstracts, 78-89.

32. Gray, D., (2002). Elastic inversion for Lame parameters Proc. of the 72th Ann Int. Meeting society Exploration Geophysicists pp 213-6
33. Weber, K.J. and E.M. Daukoru, (1975), Petroleum geology of the Niger delta: Proceedings of the 9th World Petroleum Congress, Tokyo, v. 2, p. 202-221.
34. Weber KJ (1987). Hydrocarbon Distribution Pattern in Nigeria growth fault structures controlled by structural style and stratigraphy. J. Petrol. Sci. Engine.. Elsevier Science Publishers B.V. Amsterdam, 1-12.
35. Short, K. C., and Stauble, A.J. (1967) Outline of Geology of Niger delta: American Association of Petroleum Geologists Bulletin v. 51, p. 761-779.
36. Doust, H., and E. Omatsola, (1990) Niger delta: *in* J. D. Edwards and P.A. Santogrossi, Eds. Divergent/passive margin basins: AAPG Memoir 48, p. 239-248.
37. Bahremandi, M., Mirshahani, M., Saemi, M. (2012). "Using of Compressional-Wave and Shear Wave Velocities Ratio in Recognition of Reservoir Fluid Contacts Case Study: A Southwest Iranian Oil Field" Journal of Scientific Research and Reviews. 1(2):015–019.